

## COMMUNICATION

## Glass formation via structural fragmentation of a 2D coordination network

Cite this: DOI: 10.1039/x0xx00000x

D. Umeyama,<sup>a</sup> N. P. Funnell,<sup>b</sup> M. J. Cliffe,<sup>b</sup> J. A. Hill,<sup>b</sup> A. L. Goodwin,<sup>b</sup> Y. Hijikata,<sup>c</sup> T. Itakura,<sup>d</sup> T. Okubo,<sup>e</sup> S. Horike<sup>\*a</sup> and S. Kitagawa<sup>\*a,f</sup>

Received 00th January 2012,

Accepted 00th January 2012

DOI: 10.1039/x0xx00000x

[www.rsc.org/](http://www.rsc.org/)

**The structure of a glass obtained by the melt quenching of a two-dimensional (2D) coordination network was examined. X-ray analyses disclosed a 2D-to-0D structural transformation before and after glass formation. The mechanism is unique to coordination compounds, as it is characterized by labile and flexible coordination bonds.**

Glasses are an important class of materials and can be formed by many routes. Of various routes to the glassy state, melt quenching is one of the most common methods to obtain glasses.<sup>1</sup> Many types of substances form glasses via melt quenching; there are several types of glasses classified according to their building units, including molecular (toluene), metallic (Au-Si), covalent (As<sub>2</sub>Se<sub>3</sub>), and open network glasses (SiO<sub>2</sub>).<sup>2</sup> Recently we have reported a number of melting coordination polymers (CPs), and demonstrated the glass formation of one such melting CP by melt quenching.<sup>3</sup> CPs are a class of crystalline inorganic–organic hybrids that form extended networks via coordination bonds.<sup>4</sup> The immense number of possible combinations of metal ions and ligands results in rich structural and compositional diversity in CPs. This enables fine-tuning to give CPs that can melt. In addition to the aforementioned archetypal glasses, those from molten CPs can be classified as a new type of glass former that potentially inherits the useful properties of CPs.<sup>5</sup>

Although glasses do not have long range order, the local structures often resemble those of their crystalline counterparts; therefore molecular crystals form molecular glasses, and network crystals form network glasses.<sup>6</sup> In a previous study, we examined the structure of a vitreous CP and identified that the glass state had a network structure that was similar to its crystalline state.<sup>3</sup> Other extended coordination materials, including metal–organic frameworks (MOFs), also exhibit network structures in the vitreous

states inherited from their parent crystals.<sup>7</sup> The network preservation of these materials in glass and crystalline state can be rationalized by considering the lattice enthalpies that must be comparable in both states.<sup>8</sup> However, this “preservation rule” might be expected to break down in cases where the lattice enthalpies between the two states are similar despite having very different structures.

In this communication, we report a study on a glass-forming CP, which exhibits a network-to-molecular transformation before and after glass formation. This kind of drastic fragmentation is not observed in conventional glass formers such as organic polymers and silica glasses.<sup>6</sup> The suggested molecular structure of the vitreous state, determined on the basis of X-ray absorption and pair distribution function (PDF) analyses, indicates that the chemical diversity of coordination species and flexibility in coordination geometry are responsible for the unique glass formation, which is accompanied by a dynamic rearrangement in a coordination sphere.

The glass-forming CP, [Zn(H<sub>2</sub>PO<sub>4</sub>)<sub>2</sub>(HTr)<sub>2</sub>]<sub>n</sub> (**1**; Tr: 1,2,4-triazolate), comprises octahedral (O<sub>h</sub>) zinc ions surrounded by HTr and phosphate ligands in the crystalline state. Each HTr ligand bridges two zinc ions equatorially to build an extended two-dimensional (2D) network, with the phosphate ligands standing axially on the sheet (Fig. 1a).<sup>9</sup> Air cooling at ambient temperature from the molten state of **1** is sufficiently rapid to afford the vitreous state (**1'**), suppressing the recrystallization into **1** (Fig. 1b). **1'** exhibits a glass transition at 305 K (*T<sub>g</sub>*), determined as described below using differential scanning calorimetry (DSC), and is thus stable as a glass at ambient temperature.

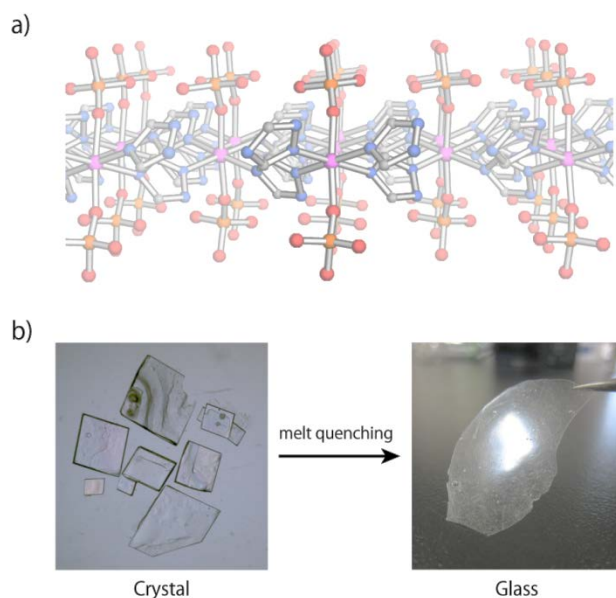


**Fig. 1** (a) Crystal structure of **1**. The Zn, P, O, N, and C atoms are shown in purple, orange, red, blue, and gray, respectively. H atoms have been omitted for clarity. (b) Photographs of the crystals of **1** and the glassy flake of **1**'.

The X-ray absorption spectra (XAS) of the K edge of the zinc ions of **1** and **1**' indicate that the arrangements around these zinc ions are distinct even at the nearest neighbors (Fig. 2). The sharp peak at the rising absorption edge — the so called “white-line” — of **1** becomes less intense in **1**'. The difference in the white-line intensities suggests a change in the site symmetries of the zinc ions (i.e., how the orbitals are hybridized) because the intensities are subject to the selection rule of electron transitions ( $\Delta l = \pm 1$ ). Besides an  $O_h$  arrangement, a zinc ion is also stable in a tetrahedral ( $T_d$ ) arrangement. The  $T_d$  arrangement is well ascribed to the less intense white line of **1**' because the electronic transitions associated with X-ray absorption at the K edge of the  $T_d$  zinc ions have a stronger character of  $1s \rightarrow 3d$  transition ( $\Delta l = + 2$ ) than those of  $O_h$ .<sup>10</sup> The radial distribution function (RDF) around the zinc ions of **1**' deduced from its XAS is fitted well by a model in which the zinc ions are surrounded by four atoms with a shorter bond distance than those of **1** (Fig. S1 and Table S1 in ESI). Therefore, we postulate that the arrangement around the zinc ions has changed from  $O_h$  to  $T_d$  during the phase transition.

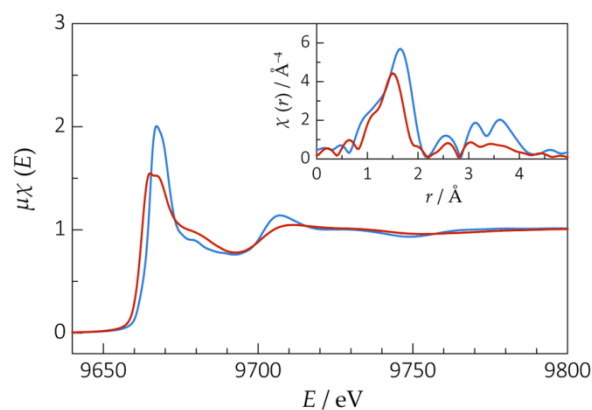


**Fig. 2** XASs of **1** (blue) and **1**' (red) observed at the K edge of the zinc atoms at 298 K and the derived RDFs (inset).

In order to probe the detailed structure of **1**', we collected X-ray total scattering data using a PANalytical Empyrean diffractometer equipped with a Ag X-ray tube. The normalized and corrected X-ray structure factors  $F(Q)$  and the corresponding pair distribution functions  $D(r)$  are given in Fig. 3.<sup>11</sup> On the basis of the  $D(r)$  of **1**, the single crystal structure of **1** was refined and thus some peaks of the  $D(r)$  were assigned (Fig. S2 in ESI). One of the remarkable features of the  $D(r)$  of **1**' is that the atomic correlations are much diminished beyond 5 Å (Fig. 3a). The Zn-Zn correlation observed at 6.4 Å in the  $D(r)$  of **1** has disappeared in that of **1**', suggestive of the absence of an extended structure in **1**' (Fig. 3b). This is in striking contrast to the PDFs of the amorphous ZIFs, for which the Zn-Zn correlation is preserved.<sup>12,7a</sup> In addition, the peak for the coordination shell of the zinc ions (around 2 Å) has a lower intensity and occurs at shorter distance for **1**' than for **1**, consistent with the  $T_d$  arrangement of the zinc ions of **1**' suggested by the XAS spectrum.

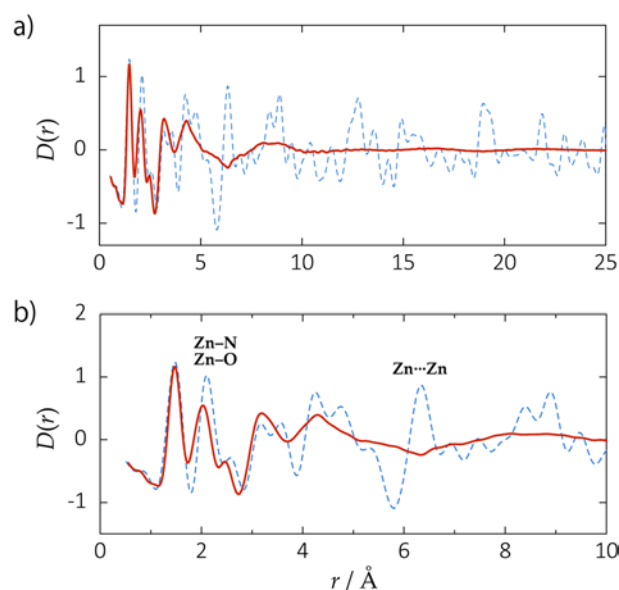


**Fig. 3** (a)  $D(r)$  of **1** (blue) and **1**' (red) at 298 K from 1 to 25 Å. (b) Comparison of the  $D(r)$ s of **1** (blue) and **1**' (red) in the range from 1 to 10 Å (298 K). Some of the assigned peaks of the  $D(r)$  of **1** are indicated.

The remarkably short correlation length evident from the PDF profile of **1'** suggests that the building unit of **1'** is likely a discrete molecule (0D).<sup>13</sup> Therefore, we built a molecular model for **1'** as shown in Fig. 4a (bottom). The model was obtained by changing the HTr molecules from bridging to monodentate ligands; thus the geometry becomes  $T_d$  while the chemical formula remains the same as **1**,  $[\text{Zn}(\text{H}_2\text{PO}_4)_2(\text{HTr})_2]$ , except that it is no longer a constitutional repeating unit. Expecting that the vitreous **1'** is a condensed phase in which  $[\text{Zn}(\text{H}_2\text{PO}_4)_2(\text{HTr})_2]$  molecules pack randomly, we constructed a  $25 \times 25 \times 25 \text{ \AA}^3$  cubic amorphous cell with  $P1$  symmetry filled with the fifty molecules by using the Amorphous Cell module implemented in Accelrys Materials Studio 6.0.<sup>14</sup> The amorphous cell was relaxed via MD simulation using the Forcite module (Fig. 4b), and whose  $2 \times 2 \times 2$  super cell was settled as an initial model for a reverse Monte Carlo (RMC)<sup>15</sup> refinement. We used the program RMCProfile and refined the structure to fit the X-ray total scattering data in real and reciprocal space (Fig 4c).<sup>16</sup> The refined structure maintained the initial MD constitution (Fig. S3 in ESI), and thus we succeeded in suggesting a consistent structural model for **1'**.

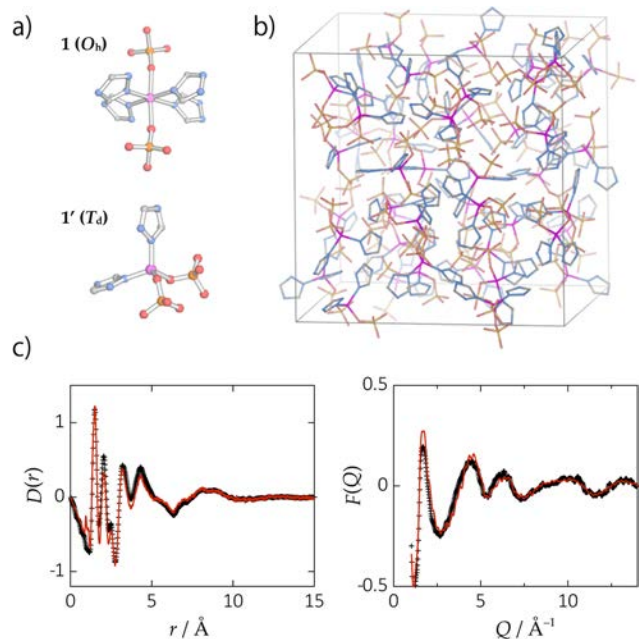


**Fig. 4** (a) Arrangements around the zinc ions for **1** (top) and **1'** (bottom, postulated). (b) Amorphous cell that comprises 50  $T_d$  models for **1'**. (c) Result of RMC refinement of the amorphous cell in real (left) and reciprocal spaces (right). Experimental data and fitting results are shown in black crosses and red lines, respectively.

Having established a viable structural model for **1'**, its physical properties are of interest. Heat capacity ( $C_p$ ) is one of the most important thermodynamic parameters to characterize glasses, and we ascribe the behavior of the  $C_p$  of **1'** to its discrete molecular structure. As shown in Fig. 5, the glass transition of **1'** is superimposed on a gradually-rising background, indicating that the molecular rearrangements involved in the glass transition commence before the vibrational heat capacity is fully excited. This is a common characteristic for molecular glass formers, which have vibrational modes in infrared and Raman regions (i.e., with high Einstein

temperatures). While thermally amorphized ZIF-4, known to be a molecular network glass, also exhibits glass transitions on the slope of  $C_p$ , the jump of the  $C_p$  at the  $T_g$  ( $\Delta C_p(T_g)$ ) of **1'** is more than four times larger ( $\Delta C_p(T_g) = 0.70 \text{ J K}^{-1} \text{ g}^{-1}$ ) than that of high density amorphous (HDA) ZIF-4 ( $\Delta C_p(T_g) = 0.16 \text{ J K}^{-1} \text{ g}^{-1}$ ).<sup>7a</sup> The small  $\Delta C_p(T_g)$  of amorphous ZIF-4 is explained by its three dimensional bonding pattern, cf. vitreous  $\text{GeO}_2$  (an inorganic network glass).<sup>1</sup> In contrast, the large  $\Delta C_p(T_g)$  of **1'** is due to its discrete structure, as seen in other molecular glass formers including toluene and ethanol.<sup>17</sup> The normalized  $C_p$  value of **1'**,  $C_p(\mathbf{1}')/C_p(\mathbf{1})$ , exceeds 2 around  $T_g$  (Fig. 5 inset). This supports the attribution of a discrete molecular structure in which the configurational heat capacity is larger than that of a network glass. The change in entropy across the glass transition was calculated as  $\Delta S(\mathbf{1}') = 81 \text{ J K}^{-1} \text{ mol}^{-1}$  (280–325 K).

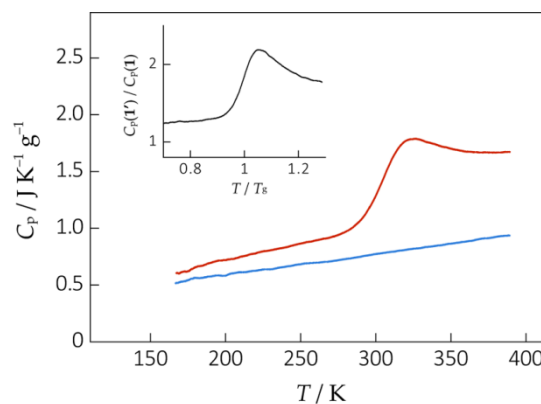


**Fig. 5** Heat capacities of **1** (blue) and **1'** (red) calculated from DSC measurements. Inset shows the variation of the heat capacity through the glass transition for **1'**.

We performed density functional theory (DFT) calculations to understand the energetics of **1** and **1'**. According to the Gibbs free energies of the complex formation reactions ( $\Delta_r G$ ) of the finite  $O_h$  and  $T_d$  models at 298 K (Fig. S4 and Scheme S1 in ESI), the energy difference between the two configurations is only  $54 \text{ kJ mol}^{-1}$  ( $\Delta_r G(O_h) = -2616 \text{ kJ mol}^{-1}$ ,  $\Delta_r G(T_d) = -2562 \text{ kJ mol}^{-1}$ ). Considering that the  $T_d$  arrangement can form more hydrogen bonds (which are not included in the DFT calculation) than the  $O_h$  arrangement, the energy difference may be less than  $54 \text{ kJ mol}^{-1}$ , and thus the small free energy difference indicated by the DFT calculations also represents the validity of the  $T_d$  model. The bistability of zinc ion in the two arrangements, combined with electrical neutrality of the bridging ligand (HTr), appear to be the keys for enabling the fragmentation into 0D structure. The structural flexibility and compositional diversity of coordination compounds are of central importance for this unique behavior. Having a permanent dipole moment (5.61 Debye; indicated by the DFT calculation), the dielectric and optical properties of **1'** are of interest for applications as a functional glass.<sup>18</sup>

## Conclusions

The disordered structures of glasses are most commonly characterized as continuous random networks (CRNs) in 3D and 2D

systems,<sup>19</sup> or entangled strings in 1D systems (linear polymers).<sup>20</sup> In this study, we examined the structure and properties of a glass obtained by melt quenching of a 2D coordination network. The XAS and PDF analyses indicated a discrete (0D) structure for the glass state which was consistent in terms of composition, preferred coordination geometries for zinc ions, behavior in heat capacity, and energetics in DFT calculations. The RMC refinement of the amorphous cell of the 0D models visualized the glass structure in bulk, elucidating a unique glass formation from 2D materials. This mechanism of glass formation is characteristic to coordination compounds in the sense that it requires labile bonds and flexible rearrangements. Having performed a structure study for a glass from 2D coordination network, in addition to 1D<sup>3</sup> and 3D<sup>7a</sup> systems, we would be able to understand an important design guide for preparing glass forming CPs. Our study provides a useful insight to developing novel functional glasses from CPs.

## Notes and references

This work was supported by the PRESTO of the Japan Science and Technology Agency (JST), and a Grant-in-Aid for Scientific Research on the Innovative Areas: "Fusion Materials", Grant-in-Aid for Young Scientists (A), Grant-in-Aid for Challenging Exploratory Research from the Ministry of Education, Culture, Sports, Science and Technology, Japan. iCeMS is supported by the World Premier International Research Initiative (WPI) of MEXT, Japan. D.U. is grateful to JSPS Research Fellowships for Young Scientists. N.P.F, M.J.C, J.A.H. and A.L.G acknowledge financial support from the E.P.S.R.C. (EP/G004528/2) and the E.R.C. (Grant Ref: 279705)

<sup>a</sup> Department of Synthetic Chemistry and Biological Chemistry, Graduate School of Engineering, Kyoto University, Katsura, Nishikyō-ku, Kyoto 615-8510, Japan.

<sup>b</sup> Inorganic Chemistry Laboratory, Department of Chemistry, University of Oxford, South Parks Road, Oxford OX1 3QR, UK.

<sup>c</sup> Institute of Transformative Bio-Molecules (WPI-ITbM), Nagoya University, Chikusa-ku, Nagoya 464-8602, Japan.

<sup>d</sup> DENSO CORPORATION, 1-1 Showa-cho, Kariya, Aichi 448-8661, Japan.

<sup>e</sup> Department of Chemistry, School of Science and Engineering, Kinki University, Kowakae, Higashi-Osaka, Osaka 577-8502, Japan.

<sup>f</sup> Institute for Integrated Cell-Material Sciences (WPI-iCeMS), Kyoto University, Yoshida, Sakyo-ku, Kyoto 606-8501, Japan.

<sup>†</sup> Electronic Supplementary Information (ESI) available: experimental details on [Zn(H<sub>2</sub>PO<sub>4</sub>)<sub>2</sub>(HTr)<sub>2</sub>]<sub>n</sub> synthesis, X-ray absorption spectra, X-ray total scattering, reverse Monte Carlo model construction and refinement, differential scanning calorimetry, and density functional theory calculations. See DOI: 10.1039/c000000x/

1 C. A. Angell, *Science*, 1995, **267**, 1924.

2 C. A. Angell, *Pure Appl. Chem.*, 1991, **63**, 1387.

3 D. Umeyama, S. Horike, M. Inukai, T. Itakura and S. Kitagawa, *J. Am. Chem. Soc.*, 2015, **137**, 864.

4 (a) B. Moulton and M. J. Zaworotko, *Chem. Rev.*, 2001, **101**, 1629; (b) L. Carlucci, G. Ciani and D. M. Proserpio, *Coord. Chem. Rev.*, 2003, **246**, 247; (c) C. Janiak, *Dalton Trans.*, 2003, 2781.

5 (a) Y. Pei, M. Verdager, O. Kahn, J. Sletten and J. P. Renard, *J. Am. Chem. Soc.*, 1986, **108**, 7428; (b) H. Kitagawa, N. Onodera, T. Sonoyama, M. Yamamoto, T. Fukawa, T. Mitani, M. Seto and Y. Maeda, *J. Am. Chem. Soc.*, 1999, **121**, 10068; (c) H. Kishida, H. Matsuzaki, H. Okamoto, T. Manabe, M. Yamashita, Y. Taguchi and Y. Tokura, *Nature*, 2000, **405**, 929; (d) S. R. Batten and K. S. Murray, *Coord. Chem. Rev.*, 2003, **246**, 103; (e) Y. Nagao, M. Fujishima, R. Ikeda, S. Kanda and H. Kitagawa, *Inorg. Chem. Commun.*, 2003, **6**, 346; (f) S. Kitagawa, R. Kitaura and S. Noro, *Angew. Chem., Int. Ed.*, 2004, **43**, 2334; (g) M. Ballesteros-Rivas, A. Ota, E. Reinheimer, A. Prosvirin, J. Valdés-Martinez and K. R. Dunbar, *Angew. Chem.*, 2011, **123**, 9877.

6 G. N. Greaves and S. Sen, *Adv. Phys.*, 2007, **56**, 1.

7 (a) T. D. Bennett, J.-C. Tan, Y. Z. Yue, C. Ducati, N. Terril, H. H. M. Yeung, Z. Zhou, W. Chen, S. Henke, A. K. Cheetham and G. N. Greaves, *ARXIV*, 2014, arXiv:1409.3980; (b) T. S. Eike, E. Edengeiser, B. Mallick, M. Havenith and A.-V. Mudring, *Chem. Eur. J.*, 2014, **20**, 5338.

8 A. B. Cairns and A. L. Goodwin, *Chem. Soc. Rev.*, 2013, **42**, 4881.

9 D. Umeyama, S. Horike, M. Inukai, T. Itakura and S. Kitagawa, *J. Am. Chem. Soc.*, 2012, **134**, 12780.

10 J. Rose, I. Moulin, A. Masion, P. M. Bertsch, M. R. Wiesner, J. Y. Bottero, F. Mosnier and C. Haehnel, *Langmuir*, 2001, **17**, 3658.

11 (a) D. A. Keen, *J. Appl. Cryst.*, 2001, **34**, 172; (b) The total scattering functions used here follow the formalisms given by reference #11(a).

12 (a) T. D. Bennett, A. L. Goodwin, M. T. Dove, D. A. Keen, M. G. Tucker, E. R. Barney, A. K. Soper, E. G. Bithell, J.-C. Tan and A. K. Cheetham, *Phys. Rev. Lett.*, 2010, **104**, 115503; (b) T. D. Bennett and A. K. Cheetham, *Acc. Chem. Res.*, 2014, **47**, 1555.

13 N. P. Funnell, M. T. Dove, A. L. Goodwin, S. Parsons and M. G. Tucker, *J. Phys.: Condens. Matter*, 2013, **25**, 454204.

14 Accelrys Software Inc., Material Studio Modeling Environment, Release 6, Accelrys Software Inc., San Diego, California, USA, 2011.

15 R. L. McGreevy and L. Pusztai, *Molecular Simulation*, 1988, **1**, 359.

16 M. G. Tucker, D. A. Keen, M. T. Dove, A. L. Goodwin and Q. Hui, *J. Phys.: Condens. Matter*, 2007, **19**, 335218.

17 C. Alba, L. E. Busse, D. J. List and C. A. Angell, *J. Chem. Phys.*, 1990, **92**, 617.

18 N. F. Borrelli and M. M. Layton, *J. Non-Cryst. Solids*, 1971, **6**, 197.

19 (a) M. G. Tucker, D. A. Keen, M. T. Dove and K. Trachenko, *J. Phys.: Condens. Matter*, 2005, **17**, S67; (b) P. Y. Huang, S. Kurasch, A. Srivastava, V. Skakalova, J. Kotakoski, A. V. Krashennikov, R. Hovden, Q. Mao, J. C. Meyer, J. Smet, D. A. Muller and U. Kaiser, *Nano Lett.*, 2012, **12**, 1081; (c) L. Lichtenstein, C. Büchner, B. Yang, S. Shaikhutdinov, M. Heyde, M. Sierka, R. Włodarczyk, J. Sauer and H.-J. Freund, *Angew. Chem., Int. Ed.*, 2012, **51**, 404.

20 (a) R. H. Colby, L. J. Fetters and W. W. Graessley, *Macromolecules*, 1987, **20**, 2226; (b) M. D. John and G. L. Ronald *Structure and Rheology of Molten Polymers*; Carl Hanser Verlag GmbH & Co. KG, **2006**.